Journal of Zhejiang University SCIENCE A
ISSN 1009-3095
http://www.zju.edu.cn/jzus
E-mail: jzus@zju.edu.cn


# Coaxial liquid-liquid flows in tubes with limited length*

HU Ying-ying (胡影影)†, HUANG Zheng-ming (黄争鸣)

(*School of Aerospace Engineering and Applied Mechanics, Tongji University, Shanghai 200092, China*)

†E-mail: huyingying@mail.tongji.edu.cn

Received Oct. 22, 2005; revision accepted Nov. 25, 2005

**Abstract:** Coaxial liquid-liquid flows were numerically studied in a nesting two-tube system. Calculations were carried out when various exit-lengths (meaning length differences between the two tubes) were used. Numerical results indicated that there exists a certain range of exit-length for the liquid-liquid flows to form stable and smooth interfaces, which requires that the exit-length should roughly be less than 5.6 times the outer tube diameter. In this range, interface instability is effectively restrained and the core fluid shows a phenomenon of die swell. When the exit-length is about 1.6 times the outer tube diameter, the core fluid has the greatest diameter size in the shell fluid. Velocity distributions at the outer tube exit favor formation of a continuous and stable core-shell structure.

**Key words:** Coaxial liquid-liquid flow, Exit-length, Instability, Die swell
**doi:**10.1631/jzus.2006.A0347 **Document code:** A **CLC number:** O357; O359

## INTRODUCTION

Having numerous engineering applications, liquid-liquid flows are an important research branch of fluid dynamics being studied (Drazin and Reid, 1981). But for coaxial liquid-liquid flows occurring in a limited tube domain, there has been little available reference.

Coaxial electrospinning composite nanofibers is one of the associated applications, where a nesting tube system is used: an inner tube is put inside an outer tube with longer length and larger diameter. Such a tube system is used to form a core-shell fluid fiber so that it may be stretched and solidified into a nanometer-scaled composite fiber after being ejected from the tubes (Sun *et al.*, 2003; Loscertales *et al.*, 2004).

Due to their unique properties, nanofibers have been widely studied (Huang *et al*., 2003; Yarin, 2003), but mainly based on experiments while their theoretical mechanism is still elusive. Viscosity of polymer liquids, surface tension, electrostatic fields, liquid polarization and free charge introduction, are all factors influencing resultant nanofibers (Hertz and Hermanrud, 1983). The non-Newtonian property of the polymer liquids is one of the greatest difficulties precluding theoretical analysis. From the point of view of fluid mechanics, more often than not, theoretical study is still in the range of Newtonian fluids or even potential flows (Reneker *et al.*, 2000; Yarin *et al.*, 2001; Reznik *et al.*, 2004; Theron *et al.*, 2004).

Most theoretical research on nanofibers is focused on nanofibers made of a single material and on the physical process of fluid fibers ejected out of tubes. When two liquids form a core-shell structure, interfaces between them involve extra difficulties and the flow process within the tubes becomes equally important for understanding the whole process of manufacturing composite nanofibers.

In view of such research conditions, we established a simplified dynamic model to numerically study the effects of tube geometry on the coaxial liquid-liquid flows occurring in the limited tube domain, where Newtonian fluid is still adopted as one of the assumptions.

*Project supported by the National Natural Science Foundations of China (No. 10402031) and the NanoSci Tech Promotion Center, the Shanghai Science & Tech. Committee (No. 0352nm091), China

## MODEL DEVELOPMENT

A schematic diagram of a two-tube system is shown in Fig.1. Two coordinate systems, the rectangular coordinates ($x$, $y$, $z$) and the cylindrical polar coordinates ($r$, $\theta$, $x$), are adopted. In Fig.1, $d_i$, $d_o$ are the inner diameters of the inner and outer tubes, and $d_w$ is the outer diameter of the inner tube. $x_i$ and $x_o$ are respectively the inner and outer tube lengths. In this study, the distance of $x_o-x_i$ is named as the exit-length.

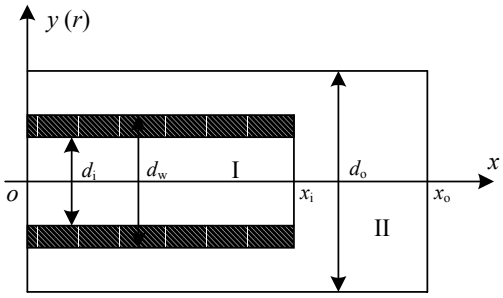


**Fig.1 Schematic arrangement of a nesting tube system (not to scale)**

Region I in Fig.1 is the whole domain enclosed by the inner tube; region II is the space within the outer tube excluding that occupied by the inner tube. At the beginning, the core fluid occupies region I whereas the shell fluid fills region II. When body forces are imposed along the tube axes, they drive fluids to move towards the exit of the outer tube. During this process, the core fluid from the inner tube enters into the shell fluid and is wrapped by the latter. We are interested in the fluid flow after it is fully developed within the tubes.

On these conditions, the governing equations for incompressible Newtonian fluids include the continuum Eq.(1) and momentum equation Eq.(2):

$$\nabla\cdot\boldsymbol{V}=0, \tag{1}$$

$$\frac{\partial \boldsymbol{V}}{\partial t}+\boldsymbol{V}\cdot\nabla\boldsymbol{V}=-\frac{1}{\rho}\nabla p+\boldsymbol{f}+\nu\nabla^2\boldsymbol{V}, \tag{2}$$

where $\boldsymbol{V}$ is a velocity vector, $p$ pressure, $\nu$ constant kinematic viscosity, $\rho$ fluid density, and $\boldsymbol{f}$ the body force vector. The derivative of the velocity vector with respect to time in Eq.(2) is nominal, from which a steady solution is expected.

Boundary conditions are specified in cylindrical polar coordinates. At the inlet $x=0$, the flow state is:

$$\boldsymbol{V}=0, \quad p=p_0, \tag{3}$$

where $p_0=1.01\times10^5$ Pa is the standard atmosphere pressure. At the exit $x=x_o$, the outflow condition is

$$\partial\boldsymbol{V}/\partial x=0,\ \partial p/\partial x=0. \tag{4}$$

On tube walls, a non-slip condition is applied:

$$\boldsymbol{V}=0. \tag{5}$$

When a large enough body force is used so that the effects of surface tension can be neglected, velocity, pressure and stresses are supposed to be continuous across interfaces. Interfaces are tracked with the volume of fluid method (Scardovelli and Zaleski, 1999; FLUENT6.0, 2003).

## RESULTS AND DISCUSSIONS

### Parameter specification

As in (Rutledge *et al*., 2001), we set densities and viscosities of the core and shell fluids respectively as $\rho_{co}$=870 kg/m$^3$, $\rho_{sh}$=1280 kg/m$^3$, $\mu_{co}$=0.011 kg/ms, and $\mu_{sh}$=0.15 kg/ms. The body force acts along the $x$-direction (Fig.1), $f_x$=1000 m/s$^2$, with the body force components $f_y$, $f_z$ being zero. Tube dimensions are: $d_i$=0.5 mm; $d_w$=0.8 mm; $d_o$=1.6 mm; $x_i$=15 mm; $x_o$=20 mm.

### Swell of the core fluid

For coaxial liquid-liquid flows in tubes, the relative cross-sectional area of the core fluid to the whole fluids is important to describe the coaxial liquid-liquid flows. Using $A_{tu}$ as the cross-sectional area of the outer tube and $A_{co}$ that of the core fluid, the relative cross-sectional area of the core fluid at the outer tube exit $x=x_o$ can be defined as the cross-sectional area ratio, $A_{co}/A_{tu}$.

Fluid flow in the coaxial tubes is axial-symmetric. Fig.2 shows the spatial distribution of the core and shell fluids on the plane of $z=0$. When fully developed, $A_{co}/A_{tu}$ is a constant 0.23. This value exists for a certain distance before the core fluid

reaches the exit (Fig.2), which makes it possible to use parameters obtained at the outer exit to gain understanding of the within tube flow.

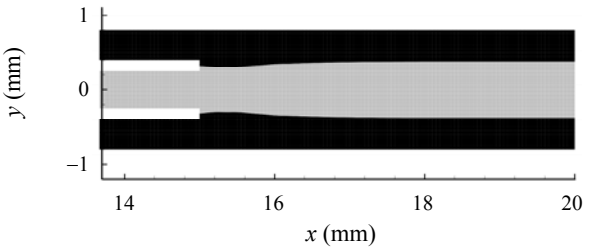


**Fig.2 Spatial distribution of the core and shell fluids on the plane $z$=0**

As the core fluid is confined within the inner tube, $A_{co}/A_{tu}$ is equal to the cross-sectional area ratio of the two tubes, 0.098, much less than $A_{co}/A_{tu}$=0.23 at the outer exit. This indicates that the core fluid diameter enlarges after the core fluid flows into the shell fluid, which is a phenomenon similar to 'die swell' occurring in non-Newtonian flows across a tube exit to the air and agrees with common knowledge that even Newtonian fluids have a certain but weak die swell effect when extruding from a narrow space (Joseph, 1990; Feng *et al.*, 1995).

Here the swell phenomenon of the core fluid can be partially explained by velocity distributions at the outer tube exit. Among three velocity components, the axial velocity is obviously dominant in magnitude. The tangential velocity is neglected due to the axial symmetry of the flow. The axial velocity is much smaller than the radial velocity and is only about $10^{-3}$ that of the axial velocity. The radial velocities of the core and shell fluids, plotted in Fig.3, strongly show sine-like functions of time. It should be noted that all velocities mentioned here are area-weighted average velocities.

Fig.3 shows three phenomena: (1) The radial velocity of the core fluid is generally positive whereas that of the shell fluid is negative; (2) The absolute radial velocity of the core fluid is greater than that of the shell fluid; (3) The two radial velocity curves are anti-phase; in other words, at a cross section, when the core fluid has a positive radial velocity component, the shell fluid has a negative one. Phenomena (1) and (2) result in larger $A_{co}/A_{tu}$ at $x=x_o$, which is about 2.3 that at $x$=0. Meanwhile, the phenomenon (3) implies that at the time when the core fluid tends to swell mostly is just the time for the shell fluid layer to be thinned mostly, and vice versa. The effect from phenomenon (3) helps to keep the core-shell structure's cross-section constant. Furthermore, the generally positive radial velocity of the core fluid and the generally negative radial velocity of the shell fluid ensure that phenomenon (3) will not lead to the core and shell fluids simultaneously becoming thin so that cavities would occur.

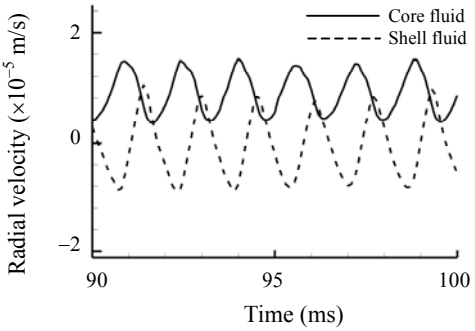


**Fig.3 Radial velocities of the core and shell fluids fluctuate at $x=x_o$**

## Effects of the exit-length

In practice, the swell effect depends on many and more direct parameters: fluid properties, tube geometry, flow conditions, etc. (Hertz and Hermanrud, 1983; Joseph, 1990). Among these, we studied tube geometry in detail first: the relationship between the cross-sectional area ratio $A_{co}/A_{tu}$ and the relative exit-length in the tube domain. For convenience, the relative exit-length is denoted by $l_e$, and defined as $l_e=(x_o-x_i)/d_o$.

Besides the relative exit-length $l_e$=3.1 used in subsection "Swell of the core fluid", more calculations were carried out when $l_e$ varied from 0 to 8.8 (during which $x_i$ changed from 0.006 m to 0.02 m while other parameters ($d_i$, $d_w$, $d_o$, $x_o$) were retained). Results in Fig.4 show, for a value of $l_e$ in the range of 0 to 5.6, $A_{co}/A_{tu}$ attains a definite value if the fluid flow had fully developed. In Fig.4, $A_{co}/A_{tu}$ sharply rises from 0.098 to 0.24 with $l_e$ growing from 0 to 1.6, during which $A_{co}/A_{tu}$ increased moderately as $l_e$ varied from 0.13 to 0.38. Afterward maximizing at 0.24 at $l_e$=1.6, $A_{co}/A_{tu}$ smoothly decreased down to 0.21 at $l_e$=5.6.

When $l_e$>5.6, however, no fixed value of $A_{co}/A_{tu}$ at the outer exit $x=x_o$ could be obtained. Fig.5 shows

the severely fluctuating curve of $A_{co}/A_{tu}$ versus time at $l_e$=8.8. The interface between the two fluids is corrugated (Fig.6). In the range of $l_e$>5.6, the greater the $l_e$, the greater the fluctuation of $A_{co}/A_{tu}$ in magnitude and the more severe the interface corrugation.

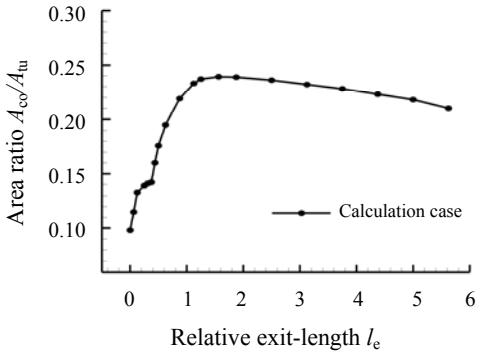


**Fig.4 The cross-sectional area ratio $A_{co}/A_{tu}$ vs the relative exit-length $l_e$**

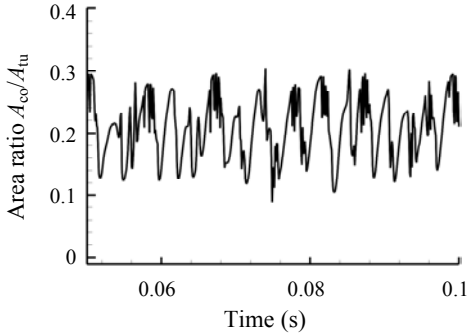


**Fig.5 At $l_e$=8.8, the cross-sectional area ratio $A_{co}/A_{tu}$ fluctuated at the outer exit $x=x_o$**

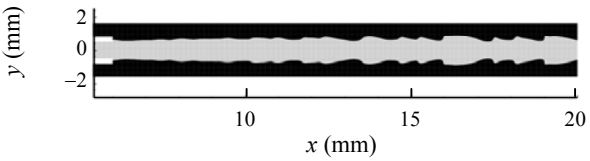


**Fig.6 At $l_e$=8.8, the spatial distribution of the core and shell fluids on the plane $z$=0**

Corrugated interface was usually observed in water-lubricated heavy oil transport, where both horizontal and vertical pipelines were used (Bai *et al.*, 1992; Arney *et al.*, 1996; Joseph, 1997). For vertical pipeline systems, the linear stability theory has been applied to explain the corrugated interfaces, also called saw-tooth waves. It was found that interface instability introduces saw-tooth waves and helps to lubricate oils in pipes (Bai *et al*., 1992).

Though instability is inherent in interface flows (Drazin and Reid, 1981), our numerical results suggested that interface instability needs certain space to develop to such a degree as to be visualized. Different from water-lubricated oil transport flow occurring in pipelines with entrance and exit effects reasonably neglected (Bai *et al.*, 1992; Arney *et al.*, 1996; Joseph, 1997), coaxial liquid-liquid flow discussed here occurs in a domain with limited flow distance. This limited space is the causative reason for the existence of a critical exit-length for interfaces to become smoothed or corrugated. When $l_e$ is less than the critical value, for example 5.6 here, interface instability is effectively restrained, resulting a smooth boundary between the core and shell fluids as plotted in Fig.2.

So, in practice, when smooth interfaces are favored, a short exit-length should be chosen. If a larger cross-sectional area ratio of the core fluid is desired, the exit-length should be short. But a certain exit-length range ought to be avoided when $A_{co}/A_{tu}$ changes too steeply to be easily controlled, as shown in Fig.4; in such a range, exit-length is less than or comparable to the diameter of the outer tube.

## CONCLUSION

Coaxial liquid-liquid flow in two nesting tubes with limited length was numerically studied. The core fluid shows the phenomenon of die swell. Compared with the averaged axial velocity at the outer tube exit, the averaged radial velocity is quite small in magnitude, but it works in a way that avoids cavities appearing between the core and shell fluids.

Interface instability inherent in liquid-liquid flow needs certain space to fully develop. To form smooth interfaces in the coaxial liquid-liquid flow, the exit-length of the tube system should be confined within a certain range, say, less than 5.6 times the outer tube diameter. In this range, when the exit-length is about 1.6 times the outer tube diameter, the core fluid can swell to the greatest degree.

## References

Arney, M.S., Ribeiro, G.S., Guevara, E., Bai, R., Joseph, D.D., 1996. Cement-lined pipes for water lubricated transport of heavy oil. *International Journal of Liquid-liquid Flow*,

**22**(2):207-221.

Bai, R., Chen, K., Joseph, D.D., 1992. Lubricated pipelining: stability of core-annular flow. Part 5. Experiments and comparison with theory. *J. Fluid Mech.*, **240**:97-132.

Drzain, P.G., Reid, W.H., 1981. Hydrodynamic Stability. Cambridge University Press.

Feng, J., Huang, P.Y., Joseph, D.D., 1995. Dynamic simulation of the motion of capsules. *J. Fluid Mech.*, **286**:201-227.

FLUENT6.0, 2003. User Guide Documentation, Computational Fluid Dynamics Software. New Hampshire, Lebanon.

Hertz, C.H., Hermanrud, B., 1983. A liquid compound jet. *J. Fluid Mech.*, **131**:271-187.

Huang, Z., Zhang, Y., Kotaki, M., Ramakrishna, S., 2003. A review on polymer nanofibers by electrospinning and their applications in nanocomposites. *Composites Science and Technology*, **63**(15):2223-2253. [doi:10.1016/S0266-3538(03)00178-7]

Joseph, D.D., 1990. Fluid Dynamics of Viscoelastic Liquids. Springer-Verlag New York Inc.

Joseph, D.D., 1997. Lubricated pipelining. *Powder Technology*, **94**(3):211-215. [doi:10.1016/S0032-5910(97)03296-8]

Loscertales, I.G., Barrero, A., Marquez, M., Spretz, R., Velarde-Ortiz, R., Larsen, G., 2004. Electrically forced coaxial nanojets for one-step hollow nanofiber design. *J. AM. CHEM. SOC.*, **126**(17):5376-5377. [doi:10.1021/ja049443j]

Reneker, D.H., Yarin, A.L., Fong, H., Koombhongse, S., 2000. Bending instability of electrically charged liquid jets of polymer solutions in electrospinning. *Journal of Applied Physics*, **87**(9):4531-4547. [doi:10.1063/1.373532]

Reznik, S.N., Yarin, A.L., Theron, A., Zussman, E., 2004. Transient and steady shapes of droplets attached to a surface in a strong electric field. *J. Fluid Mech.*, **516**:349-377. [doi:10.1017/S0022112004000679]

Rutledge, G.C., Shin, M.Y., Warner, S.B., Buer, B., Grimler, M., Ugbolue, S.C., 2001. A Fundamental Investigation of the Formation and Properties of Electrospun Fibers. National Textile Center Annual Report, M98-D01.

Scardovelli, R., Zaleski, S., 1999. Direct numerical simulation of free-surface and interfacial flow. *Annual Review of Fluid Mechanics*, **31**(1):567-603. [doi:10.1146/annurev.fluid.31.1.567]

Sun, Z., Zussman, E., Yarin, A.L., Wendorff, J.H., Greiner, A., 2003. Compound core-shell polymer nanofibers by co-electrospinning. *Advanced Materials*, **15**(22):1929-1932. [doi:10.1002/adma.200305136]

Theron, S.A., Zussman, E., Yarin, A.L., 2004. Experimental investigation of the governing parameters in the electrospinning of polymer solutions. *Polymer*, **45**(6):2017-2030. [doi:10.1016/j.polymer.2004.01.024]

Yarin, A.L., 2003. Lecture Notes 5: Electrospinning of Nanofibers from Polymer Solutions and Melts. Institute of Fundamental Technological Research, Polish Academy of Sciences, Warsaw, Poland.

Yarin, A.L., Koombhongse, S., Reneker, D.H., 2001. Bending instability in electrospinning of nanofibers. *Journal of Applied Physics*, **89**(5):3018-3026. [doi:10.1063/1.1333035]